A Directional Borehole Radar:
Numerical and Experimental Verification [1]

Koen W.A. van Dongen*, Peter M. van den Berg‡ and Jacob T. Fokkema‡

* T&A RADAR, Badhuisweg 3, PO Box 37060, 1030 AB Amsterdam, The Netherlands, email: vandongen@ta-radar.nl

‡ Centre for Technical Geoscience, Delft University of Technology, PO Box 5031, 2600 GA Delft, The Netherlands

1. Introduction

In this paper we present the simulation and design of an antenna system for a borehole radar. To obtain a directional radiation pattern the transmitting dipole is shielded with a reflector. The generated transient wavefield, with a centre frequency of 100 MHz, is reflected in the desired direction by a perfectly conducting cylindrically curved plate. The radiation pattern of this scattered wavefield is computed by solving the integral equation for the unknown electric surface current at the reflector. The reflector can have either a circular cylindrical shape or a parabolic cylindrical shape. Once the electric current distributions at the dipole and the reflector are known, the radiated wavefield can be represented by an integral over the wire and the curved plate. A prototype has been built and the simulated data are compared with experimental results.

2. Antenna configuration

An incident wavefield from an electric dipole is scattered by a perfectly conducting cylindrically curved plate with an area $\mathbb{A}$. This plate may be either circular cylindrical or parabolic cylindrical. We therefore define the domain $\mathbb{A}$ in a general orthogonal cylindrical coordinate system as,

$$\mathbb{A} = \{v_k \in \mathbb{R}^3 | -c_1 < v_1 < c_1, v_2 = c_2, -c_3 < v_3 < c_3\} \ , \qquad (1)$$

see Figure 1. In this system the components of a vector $\mathbf{u}$ is denoted as u_{v_i}, where as in the Cartesian system these are written as u_{x_i}. Consequently,

[1] published at: *2001 IEEE AP-S, International Symposium and USNC/URSI National Radio Science Meeting, Boston MA, USA, July 8-13, 2001, Vol. II, ISBN 0-7803-7070-8, pp. 746-749.*

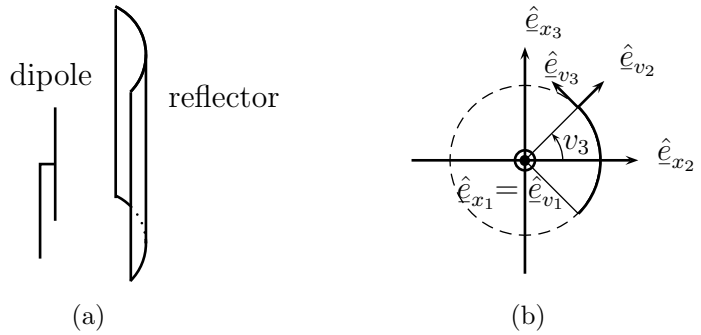

Figure 1: (a) The antenna configuration and (b) the coordinate systems.

a matrix T can be defined as the matrix which transforms quantities from the cylindrical into the Cartesian system and T^{-1} as the inverse.

The plate is embedded in a homogeneous background medium, with permittivity ε, permeability μ and electrical conductivity σ. The analysis is carried out in the frequency domain with temporal Laplace transform parameter $s = -\mathrm{i}\omega$.

3. Integral equation

The scattered wavefield, $E_i^{\mathrm{sct}}(v_k)$, is defined as the difference between the total wavefield, $E_i(v_k)$, and the incident wavefield, $E_i^{\mathrm{inc}}(v_k)$, and is represented by

$$E_{x_i}^{\mathrm{sct}}(v_k) = \frac{1}{s\varepsilon}\big(-\gamma^2\delta_{i,j} + \partial_{x_i}\partial_{x_j}\cdot\big)\int_{v_k'\in\mathbb{A}} G(v_k|v_k')J_{x_j,T}(v_k')\mathrm{d}\mathbb{A}\ . \qquad (2)$$

Here $\gamma^2 = s(s\varepsilon+\sigma)\mu$, $\delta_{i,j}$ the Kronecker delta tensor, $\partial_{x_i}\partial_{x_j}\cdot$ the gradient-divergent operator, $G(v_k|v_k')$ is the free-space Green function, and $J_{x_j,T}(v_k')$ the electric volume current density for $v_k' \in \mathbb{A}$. The subscript T is added to emphasise that only components tangential to the surface of the plate domain $\mathbb{A}$ are used.

At the surface of the reflector $\mathbb{A}$, the boundary conditions require that tangential components of the electric field vector vanish. Together with the definitions of the transformation matrices, we then obtain the integral equation,

$$-E_{v_\alpha,T}^{\mathrm{inc}}(v_k) = \frac{1}{s\varepsilon}\big(-\gamma^2\delta_{\alpha,j}+\partial_{v_\alpha,T}\partial_{v_j}\cdot\big)\mathsf{T}_{jm}^{-1}\int_{v_k'\in\mathbb{A}} G(v_k|v_k')\mathsf{T}_{m\beta}J_{v_\beta,T}(v_k')\mathrm{d}\mathbb{A}, \quad (3)$$

with $E_{v_\alpha,T}^{\mathrm{inc}}(v_k) = \{E_{v_1}^{\mathrm{inc}}(v_k), E_{v_3}^{\mathrm{inc}}(v_k)\}$ and $J_{v_\beta,T}(v_k) = \{J_{v_1}(v_k), J_{v_3}(v_k)\}$, for $\{v_k, v_k'\} \in \mathbb{A}$. Note that we have used Einstein's summation convention, where the Greek indices α and β can only be one or three. Note that integral equation (3) contains only two unknowns, $J_{v_1}(v_k)$ and $J_{v_3}(v_k)$, while $E_{v_1}^{\mathrm{inc}}(v_k)$ and $E_{v_3}^{\mathrm{inc}}(v_k)$ are known.

4. Numerical Solution of the integral equation

Integral equation (3) can be solved numerically using a standard Conjugate Gradient (CG) FFT method [Zwamborn and Van den Berg, IEEE MTT, 39, 953-960, 1991]. Consequently, the domain $\mathbb{A}$ is discretised in $(2M+1)\times(2N+1)$ equally spaced meshes of size $\Delta\mathbb{A}$. Further the following operator notation is used,

$$(Lu)_{v_\alpha;m,n} = f_{v_\alpha;m,n} \ , \tag{4}$$

where the quantities $u_{v_\alpha;m,n}$ and $f_{v_\alpha;m,n}$ are the discrete surface current values and the discrete incident electric field values, respectively, viz.,

$$u_{v_\alpha;m,n} = J_{v_\alpha,T;m,n} \qquad f_{v_i;m,n} = E^{\rm inc}_{v_\alpha,T;m,n} \ . \tag{5}$$

The operator $(Lu)_{v_\alpha;m,n}$ follows directly from equation (3). The adjoint of the operator $(Lu)_{v_\alpha;m,n}$ is defined through the inproduct of two vectors,

$$\langle r_{v_\alpha}, (Lj)_{v_\alpha}\rangle_{\mathbb{A}} = \langle (L^\star r)_{v_\alpha}, j_{v_\alpha}\rangle_{\mathbb{A}} \ , \tag{6}$$

which can be obtained by introducing the norm of two vectors v_α as,

$$\|v_\alpha\|^2_{\mathbb{A}} = \langle v_{v_\alpha}, v_{v_\alpha}\rangle_{\mathbb{A}} = \sum_{p,q}(v_{v_1;p,q}\overline{v}_{v_1;p,q} + v_{v_3;p,q}\overline{v}_{v_3;p,q})\Delta\mathbb{A} \ , \tag{7}$$

where the overbar denotes the complex conjugate. With the above definitions we are now able to apply a CG FFT iterative scheme to solve the equations. Once the normalized error ERR is small enough,

$$ERR = \frac{\|(Lj)_{v_\alpha} - E^{\rm inc}_{v_\alpha}\|_{\mathbb{A}}}{\|E^{\rm inc}_{v_\alpha}\|_{\mathbb{A}}} \ , \tag{8}$$

the approximate solution, $j_{v_\alpha} = (J_{v_1;m,n}, J_{v_3;m,n})$, may be used to calculate the scattered electric wavefield in all space via equation (2).

5. Results and discussion

In order to obtain an 'optimal' directional antenna configuration, we have carried out a number of computations. For the case where the reflector is circular cylindrical we have found an 'optimal' configuration which has been prototyped. For this configuration, the measured results will be compared with the computed ones.

For this particular configuration, the electric dipole has a length of 0.16 m, while the reflector has dimensions of 0.32 m in the direction parallel to the dipole axis and 0.11 m in the angular direction. The reflector is located at a distance of 0.09 m from the dipole axis. This antenna system is embedded in fresh water. In the computations we have taken the medium to be a non-conducting medium with a relative permittivity of 80 and a relative permeability of one. We assume a cosine-shaped electric current

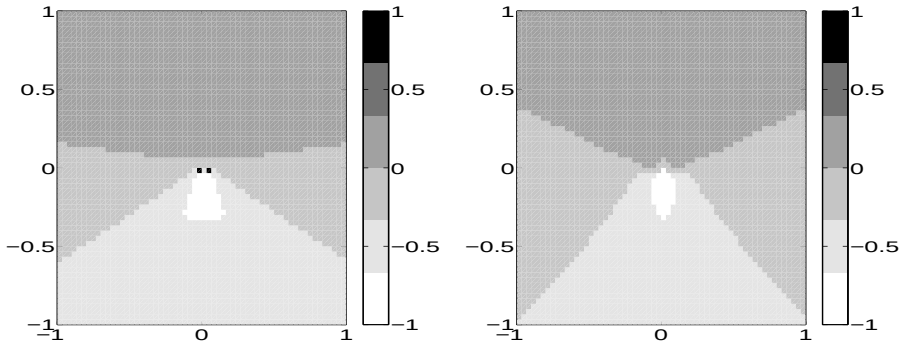

Figure 2: The radiation pattern at $x_1 = 0$ (*left*) and $x_3 = 0$ (*right*).

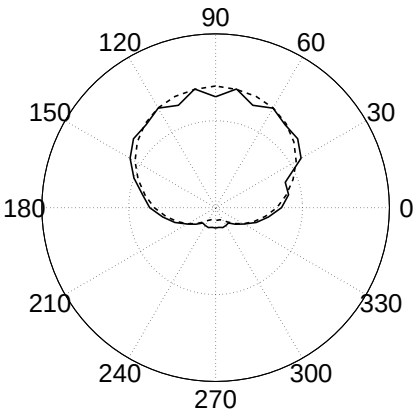

Figure 3: The radiation pattern measured (*solid line*) and computed (*dashed line*) in the plane at $x_1 = 0$ for fixed radial distance of $v_3 = 0.30$ m.

distribution, with maximum amplitude in the center and zero at both ends of the dipole. The reflector is discretised into 24 elements in the dipole direction and 16 elements in the angular direction. The iterative process is stopped as soon as the normalised error is $ERR < 0.01$.

In Figure 2 the computed radiation pattern, $^{10}\log(\|E\|/\|E^{\text{inc}}\|)$, in the plane $x_1 = 0$ and in plane $x_3 = 0$ are plotted. In Figure 3 the measured radiation characteristic (solid line) and the computed one (dashed lined) are shown. The electric field was measured with a 100 MHz electric dipole antenna in the plane $x_1 = 0$ and $v_2 = 0.30$ m. Both measurements (voltages) and computations (electric field) are normalized with a constant factor, such that the least-square differences between the measured and computed quantities are minimized. Note the excellent agreement of the two results.

From our results we conclude that, even in the low-frequency range, a directional radiation pattern can be achieved by shielding an electric dipole antenna by an appropriately designed reflector. In the low-frequency range, the electric dipole is located outside the focal point of this reflector.